

Research Journal of Pharmaceutical, Biological and Chemical Sciences

Elucidation of the Mode of Action of New Antibacterial Bis-Phosphonium Salts of Pyridine Derivatives Active Against *Staphylococcus aureus*.

Elena V. Nikitina*, Marina I. Zeldi, Rozalia M. Vafina, Mikhail V. Pugachev, Nikita V. Shtyrlin, Svetlana V. Kuznetsova, Vladimir G. Evtugyn, Airat R. Kayumov, and Yurii G. Shtyrlin¹.

Kazan (Volga Region) Federal University, Kazan, 420008, Russia.

ABSTRACT

In this study, we show the antibacterial activity of a new group of antimicrobial compounds, quaternary bis-phosphonium salts of pyridine derivatives synthesized previously in our group. These compounds exhibit broad-spectrum of antibacterial activity against gram-positive bacteria including methicillin-resistant strains of *Staphylococcus aureus*. By using both scanning and transmission electron microscopy we found that the lead compound 6-Bis[(tri-*p*-tolylphosphonio)methyl]-3-hydroxypyridin-1-ium trichloride (**2a**) bearing two *p*-tolyl substituents at the phosphorus atoms exhibits a highest antibacterial activity and affects the cell wall of *S. aureus*, which results in filamentous growth, roughened surface of cells with excrescences and unusual protrusions. While the confocal scanning microscopy showed only partial loss of membrane integrity at 1×MIC of **2a**, TEM studies revealed that **2a** exerts cell wall damage resulting in breaks and diffuse structure of peptidoglycan layer, which is likely the primary cause of its antibacterial activity. In conclusion, we suggest that the bis-phosphonium salt of pyridine with two *p*-tolyl substituents at the phosphorus atoms exert the antimicrobial activity by causing cell wall damage, making this chemotype a promising starting point for the development of new antibacterial therapies.

Keywords: quaternary phosphonium salts, pyridine, antibacterial activity, microscopy

*Corresponding author

INTRODUCTION

The wide distribution of multidrug resistant bacteria is a daunting challenge in design of new antimicrobial compounds - antibiotics, disinfectants and antiseptics. The chemical modification of different cellular metabolites or established antimicrobials is one of the promising strategies in antibacterial drug discovery [for review see 1].

Among the numerous classes of synthetic antimicrobials identified so far, the phosphonium salts of low-molecular or polymeric compounds which demonstrate promising antiviral, antibacterial, anticancer and antiparasitic properties [2 -7] are actively studied. Recently, we have reported the synthesis of novel quaternary phosphonium and bis-phosphonium salts of pyridoxine and its 6-hydroxymethyl derivatives with high antimicrobial activity against gram-positive bacteria *Staphylococcus aureus* (including MRSA strains) and *Staphylococcus epidermidis* with MIC values in the range of 1-5 µg/ml [8,9]. The quaternary phosphonium salts of pyridine carrying tolyl moieties in their structures exhibit high antibacterial activity comparable with that of vancomycin [10]. While the positively charged quaternary phosphonium and ammonium salts are believed to interact with the negatively charged cell wall of bacterial cells thus damaging the membrane function [reviewed in 11], only a small part of such compounds possess expressed antimicrobial activity. The purpose of this work was to study the mechanism of action and structure-activity relationships for these interesting antibacterial agents. Specifically, our aim was to demonstrate that introduction of p-tolyl substitutes into phosphonium salts significantly increases their antimicrobial activity, and that the active compounds exert their antimicrobial activity by causing cell wall damage.

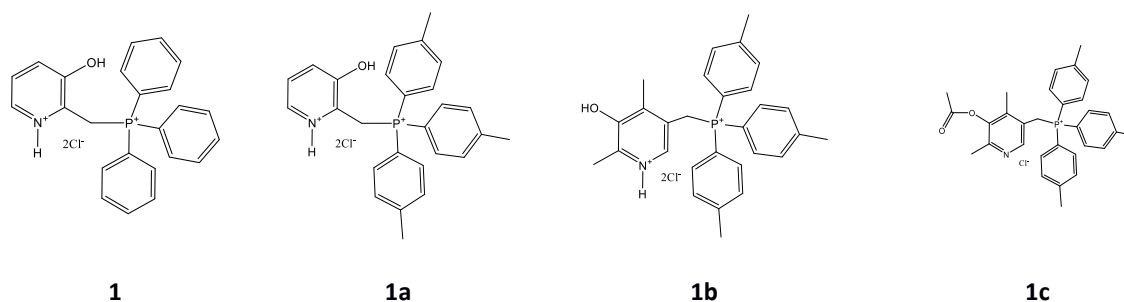
MATERIAL AND METHODS

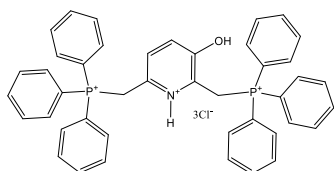
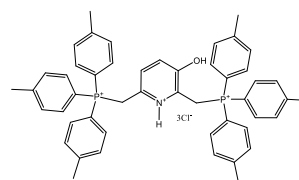
Chemical compounds, bacterial strains and growth conditions

The studied quaternary bis-phosphonium salts (see Fig.1, 1 - 2-[(Triphenylphosphonio)methyl]-3-hydroxypyridin-1-ium dichloride, 1a - 2-[(Tri-p-tolylphosphonio)methyl]-3-hydroxypyridin-1-ium dichloride, 1b - 5-[(Tri-p-tolylphosphonio)methyl]-3-hydroxy-2,4-dimethylpyridin-1-ium dichloride, 1c - 3-Acetoxy-5-[(tri-p-tolylphosphonio)methyl]-2,4-dimethylpyridin-1-ium chloride, 2 - 2,6-Bis[(triphenylphosphonio)methyl]-3-hydroxypyridin-1-ium trichloride, 2a - 6-Bis[(tri-p-tolylphosphonio)methyl]-3-hydroxypyridin-1-ium trichloride) were synthesized according to literature methods ([10]). Stock solutions of the test compounds, vancomycin, ciprofloxacin, cefazolin, and myramistin in water were sterilized by filtration through a 0.22 µm filter.

Gram-positive bacteria (*Staphylococcus aureus* ATCC® 29213™ and MRSA strains, *Staphylococcus epidermidis* (clinical isolate), *Bacillus subtilis* 168) and gram-negative bacteria (*Pseudomonas aeruginosa* ATCC® 27853™, *Klebsiella pneumoniae* (clinical isolate)) were used as test organisms. Clinical isolates of *Staphylococcus epidermidis* and *Klebsiella pneumoniae* were obtained from the Kazan Institute of Epidemiology and Microbiology (Kazan, Russia). Clinical methicillin-resistant strains of *Staphylococcus intermedius* 1143 MRSI, *S. aureus* 1134 MRSA, *S. aureus* 1145 MRSA, *S. aureus* 1131 MRSA, *S. aureus* 1130 MRSA, *S. intermedius* 1061 MRSI, *S. aureus* 1065 MRSA, *S. aureus* 1168 MRSA, *S. aureus* 1167 MRSA, *S. aureus* 2020 MRSA were obtained from patients with bronchopulmonary diseases in laboratory of bacteriology of the Republic clinical hospital (Kazan, Russia).

Fig.1. Chemical structures of the phosphonium salts of pyridine derivatives




2

2a

All the bacterial strains were maintained and cultured in a LB medium (10.0 g/L of tripton; 5 g/L of yeast extract; 5 g/L of NaCl; pH 7.0-7.2), *Staphylococci* were cultured in the Mueller-Hinton broth (Fluka).

Determination of the minimal inhibitory (MIC) and bactericidal (MBC) concentrations

The MICs of compounds were determined by the broth microdilution method in Müller-Hinton (MH) broth (pH=7.3). The compounds were diluted in a 96-well microtiter plate to final concentrations ranging from 0.5 to 1024 µg/ml in 250-µl aliquot of the bacterial suspension (5×10^5 CFU/ml) followed by their incubation at 37 °C. The MIC was determined as the lowest concentration of compound for which no visible bacterial growth could be observed after 24 h of incubation. To determine the minimum bactericidal concentration (MBC), 5 µl of culture liquid from wells with no visible bacterial growth were inoculated into 5 ml of MH broth and cultivated for 24 h. The MBC was determined as the lowest concentration of compound for which no visible bacterial growth could be observed.

Time-kill curves

The 24h-cultures of *S. aureus* ATCC 29213 were diluted 1:10000 by the fresh, preheated to 37 °C MH broth containing MIC, 1×MBC or 2×MBC of the compound followed by their incubation with agitation at 37 °C. Samples were taken each 2 h during 24 h incubation period. A 5 µl aliquote of the cell suspension was added to 500 µl of sterile 0.9% NaCl solution, the resulting solution was spread on the LB-plate surface, and CFUs were counted.

Dehydrogenase activity assay

The dehydrogenase activity was measured by using a method described earlier [12,13] with some modifications. Briefly, *S. aureus* ATCC 29213 were grown in MH broth until late exponential growth phase, harvested by centrifugation and resuspended in equal volume of 0.9% NaCl. *S. aureus* suspension (0.5 mL) and solution of the tested compound in water (0.5 mL) were placed into the Thunberg tube. The tubes were incubated at 37 °C at static conditions for 6 h. Then 0.8 mL of phosphate buffer (0.2 M, pH 7.4) and 0.5 mL of 1% glucose solution in water were added. Methylene blue (0.2 mL, 0.008% solution in water) was placed in the stopper of the Thunberg tubes, and the air was evacuated during 2 min at about 1 Torr. After 2 min preheating at 37 °C, the methylene blue and the reaction mixture were mixed to begin the reaction. After 24 h incubation at 37 °C, the optical density was measured at 610 nm. As a control, 0.9% NaCl was used instead of the compounds. The dehydrogenase activity in these tubes was considered as 100%.

Confocal laser scanning microscopy (CLSM)

Differential fluorescent staining was used to identify cells with intact and perforated membranes [14]. Cells were grown for 24 h in the presence of compound **2a** at concentrations as indicated, then harvested and washed with 0.9% NaCl. The samples were stained for 15 min with the acridine orange (green fluorescent) and propidium iodide (red fluorescent) to differentiate between undamaged and membrane-damaged bacteria, and visualized by CLMS on an inverted Carl Zeiss LSM 780 confocal laser-scanning microscope (Carl Zeiss, Jena, Germany).

Scanning electron microscopy (SEM)

For the scanning electron microscopy, the cell exposed for 24 h to antimicrobials were harvested, washed by 0.9% NaCl and fixed for 1 h in 1% glutaraldehyde. After dehydration in ethanol solutions (30, 50, 70, 80, 90, 100%), a small drop of the suspension was mounted onto a glass slide, air-dried and coated with Au/Pd (Quorum Q150T ES vacuum coater). The images were obtained by using the scanning electron microscope Merlin (Carl Zeiss, Jena, Germany), operating at an accelerating voltage of 15 kV, SE-detector.

Transmission electron microscopy (TEM)

For the transmission electron microscopy, cells were grown in Mueller Hinton broth until late exponential growth phase, harvested with centrifugation and resuspended in 0.2 Na-K phosphate buffer, pH 7.4 containing additional 1% glucose and **2a** at MIC, 1×MBC and 2×MBC. After 24 h incubation, cells were harvested and imaged.

For the transmission electron microscopy the cells were prepared by using standard protocol [15] with minor modifications. Briefly, cells were washed with saline solution twice, and fixed for 12 h in 1% glutaraldehyde solution in PBS (0.1 M sodium phosphate, 0.15 M NaCl, pH 7.4). Cell were washed twice with PBS and then incubated for 2 h in 1% OsO₄ in 0.1M PBS at room temperature. After washing, cells were dehydrated in an ethanol series (2 times in 50% ethanol for 10 min, 2 times in 70% ethanol for 10 min, 2 times in 95% ethanol for 10 min, and 3 times in 100% ethanol for 10 min) with final treatment by pure acetone for 10 min. The dehydrated samples were embedded into EPON 812 resin (Fluka Chemie AG, Switzerland), after complete polymerization the blocks were cut into thin (~1-3 μm) and ultrathin (~80-100 nm) sections with an ultramicrotome Leica EM UC7 (Leica, Germany). The thin sections were analyzed with Nikon ECLIPSE TS100 Light Microscope (Nikon, Japan) in phase contrast mode. Ultrathin sections were transferred to 3mm copper support grids (300 mesh), and imaged without uranyl acetate and lead citrate contrasting using a Transmission Electron Microscope Hitachi HT 7700 Excellence (Hitachi, Japan) operated at 80 kV in a special high contrast mode.

Statistics

All biological experiments were performed in triplicate, with three repeats. The data from the dehydrogenase assay were compared with a control using the Wilcoxon signed-rank test (a paired difference test). Differences were considered significant at $P < 0.05$. The fraction of non-viable cells was estimated as a relative number of red cells in the combined images obtained by overlaying the green and the red fluorescence microphotographs of 10 fields of view in each experiment.

RESULTS

Antibacterial activity

The antibacterial activity of the mono- and bisphosphonium salts of pyridine was studied on different gram-positive and gram-negative bacteria (Table 1). While compound **1** was inactive, the replacement of phenyl radical by *p*-tolyl (**1a**) led to an expressed antibacterial activity. Modification of pyridine ring by methylation (**1b**) or acylation (**1c**) of the phenolic hydroxyl group as well as addition of a second quaternary phosphonium group (**2**) did not improve the activity. By contrast, the substitution of phenyl by *p*-tolyl group led to significant increase in antimicrobial activity against gram-positive bacteria cells indicating that *p*-tolyl moiety is an essential pharmacophore fragment for this class of antimicrobial agents. Interestingly, neither *K. pneumonia* nor *P. aeruginosa* were affected by **2a**, indicating that gram-positive bacteria are primary target pathogens for this agent.

The activity of compounds was also tested on clinical MRSA strains sensitive to vancomycin and resistant to ciprofloxacin and cefazolin according to EUCAST statistics (Table 1). While compounds **1**, **1a**, **1b**, **1c** and **2** had the MIC values comparable with cefazolin, **2a** demonstrated the activity level against all the tested MRSA similar to that of ciprofloxacin (16-32 μg/ml vs 8-32 μg/ml, respectively) thus demonstrating a very promising antimicrobial potential.

Table 1 - Antibacterial activity mono- and bisphosphonium salt of pyridine derivatives

Strains	MIC ($\mu\text{g/ml}$) of compounds									
	1	1a	1b	1c	2	2a	Vancomycin	Ciprofloxacin	Cefazolin	Myramystyn
<i>S. aureus</i> ATCC 29213	1024	128	256	64	128	4	2	64	0.25	16
<i>S. epidermidis</i>	512	16	64	64	128	0.5	2	16	2	8
<i>B. subtilis</i> 168	1024	64	256	64	256	4	2	0.125	0.25	2
<i>K. pneumoniae</i>	1024	>1024	256	>1024	>1024	256	>1024	0.5	128	128
<i>P. aeruginosa</i> ATCC 27853	1024	>1024	256	>1024	>1024	256	>1024	2	128	128
Clinical strains										
<i>S. intermedius</i> 1143 MRSA	>1024	256	512	256	512	32	1	32	512	8
<i>S. aureus</i> 1134 MRSA	>1024	256	512	256	512	16	1	16	256	8
<i>S. aureus</i> 1145 MRSA	>1024	256	512	256	512	16	1	16	256	8
<i>S. aureus</i> 1131 MRSA	>1024	256	512	256	512	16	0.5	16	256	4
<i>S. aureus</i> 1130 MRSA	>1024	256	512	256	512	16	1	8	128	4
<i>S. intermedius</i> 1061 MRSA	>1024	256	512	256	256	32	0.5	8	256	8
<i>S. aureus</i> 1065 MRSA	>1024	256	512	256	512	32	1	16	256	8
<i>S. aureus</i> 1168 MRSA	>1024	128	256	256	256	2	0.5	0.5	0.5	8
<i>S. aureus</i> 1167 MRSA	>1024	256	512	256	512	32	0.5	16	512	4
<i>S. aureus</i> 2020 MRSA	>1024	128	256	256	256	32	0.5	0.5	1	8

Time-kill curves

For in-depth investigation of activity of **2a**, the time-kill curves were built and analyzed using *S. aureus* ATCC 29213 as model cells. Because of unknown genotype of *S. epidermidis* clinical isolate and sporulation of *B. subtilis* 168 under sublethal concentrations of antimicrobials, these bacteria were out of further investigations to avoid uncertain results. When growing in MH broth in the presence of **2a** at MIC (4 µg/ml), an amount of CFUs of *S. aureus* ATCC 29213 was reduced twice in 24 h (Fig. 2). The exposition to 1×MBC (32 µg/ml) or 2×MBC (64 µg/ml) led to complete death of cells after 9 and 6 h, respectively (Fig 2).

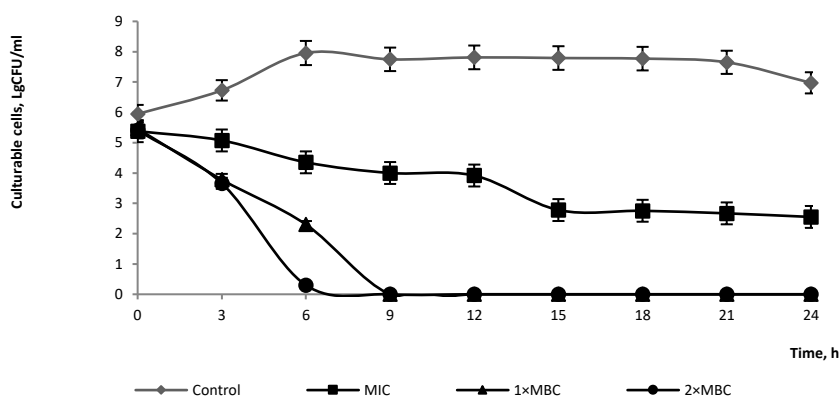


Fig.2. Time-kill curves of *S. aureus* ATCC 29213 exposed to 6-Bis[(tri-p-tolylphosphonio)methyl]-3-hydroxypyridin-1-ium trichloride (2a**) at various concentrations (MIC, 1×MBC and 2×MBC)**

Dehydrogenase activity in the presence of **2a**

Dehydrogenase enzymes, a part of glycolysis pathway of bacterial respiration, oxidize glucose in the presence of nicotinamide adenine dinucleotide (NAD), which contains a di-phosphopyridine fragment. Because of structural similarity of NAD and the studied compounds, we suggested the inhibition of dehydrogenases as possible mechanism of activity of these compounds. The activity of dehydrogenases was measured *in situ* in *S. aureus* ATCC 29213 cells exposed to different concentrations of **2a** (Fig. 3). The significant breakdown of activity was observed at concentrations of **2a** higher than 16 µg/ml, which is comparable with 1×MBC and four times higher than MIC thus indicating that dehydrogenases are not a target for this agent.

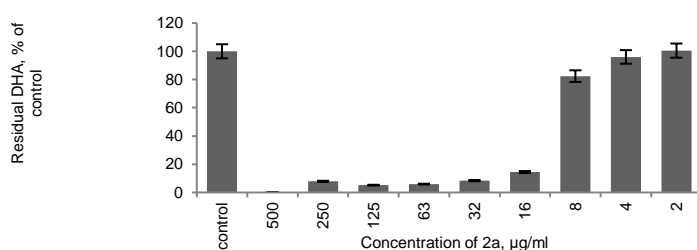


Fig. 3. Dehydrogenase activity of *S. aureus* ATCC 29213 cells after 6 h exposition to **2a (6-Bis[(tri-p-tolylphosphonio)methyl]-3-hydroxypyridin-1-ium trichloride)**

Fluorescence microscopy

Since the phosphonium salts are believed to kill bacterial cell by damaging the cell wall or cell membrane [11], we examined the membrane integrity of cells exposed to **2a**. Cells were grown until late exponential growth phase, and **2a** was added until 1×MIC, 1×MBC and 2×MBC. After 24 h of incubation, cells were harvested, washed and stained with propidium iodide and acridine orange as described in [14] and imaged by using confocal laser scanning microscopy (Fig 4). At 1×MIC of **2a**, a half of cells became red thus

indicating that cell membrane was perforated (Fig. 4B). At 1×MBC of **2a**, about 81% of cells were identified as dead (Fig. 4C), while 2×MBC led to membrane damage of 100% of cells (Fig. 4D).

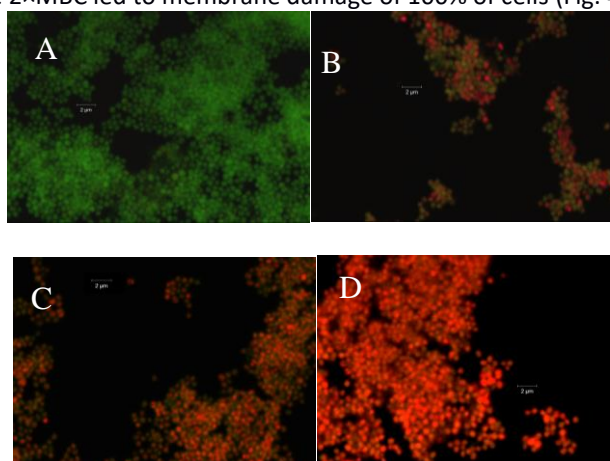
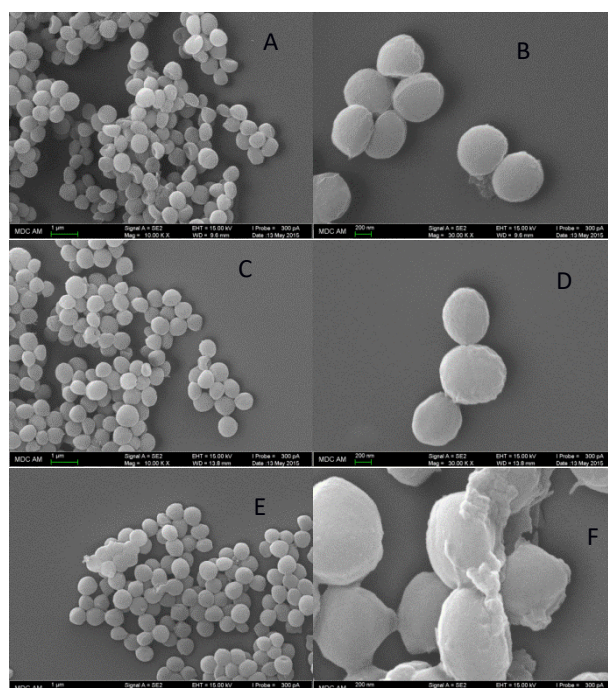


Fig. 4. Fluorescent confocal microscopy of *S. aureus* ATCC 29213 after 24 hours of exposition to the compound **2a (6-Bis[(tri-p-tolylphosphonio)methyl]-3-hydroxypyridin-1-ium trichloride) in nutrient broth and treatment with propidium iodide and acridine orange. (A) No compounds; (B) MIC of **2a**; (C) 1×MBC of **2a**; and (D) 2×MBC of **2a**. The bar corresponds to 2 μm**

SEM microscopy

Additional to CLSM, the morphological changes of cell surfaces in the presence of **2a** were investigated with scanning electron microscopy. The intact cells (Fig. 5 A, B) look like typical *Staphylococci* – spherical, smooth, and dividing in all directions. In the presence of **2a** at 1×MIC, the fraction of dividing cells is drastically reduced (Fig. 5C). The cells are characterized by the roughened surface with excrescences and unusual protrusions (Fig. 5 D). Also, the filamentous growth was observed, that is unspecific for staphylococcal cells. The exposition to 1×MBC and 2×MBC of **2a** led to changes in cell shape and pronounced filamentous growth and chains formation. As well, intensive accumulation of organic material on cell surfaces leading to cell to cell adhesion, antler-like protrusions, elongated linear cells and deep web-like fissures were observed (Fig. 5 E-H).



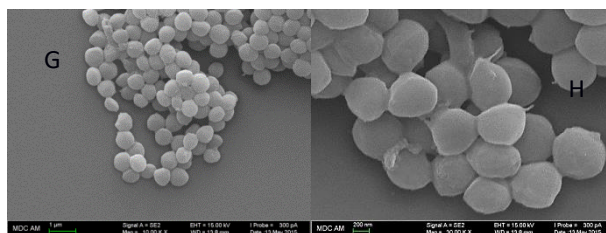


Fig.5. Scanning electron microscopy (SEM) of *S. aureus* ATCC 29213 after 24 hours exposition to 2a (6-Bis[(tri-p-tolylphosphonio)methyl]-3-hydroxypyridin-1-ium trichloride). A, B – no compounds; C, D – MIC; E, F – MBC; G, H – 2×MBC. The magnification of A, C, E, G is 10000, magnification of B, D, H is 30000, magnification of F is 50000

TEM microscopy

For deeper insight into cell morphology changes in presence of **2a**, the treated and non-treated cells were also analyzed by transmission electron microscopy (Fig. 6).

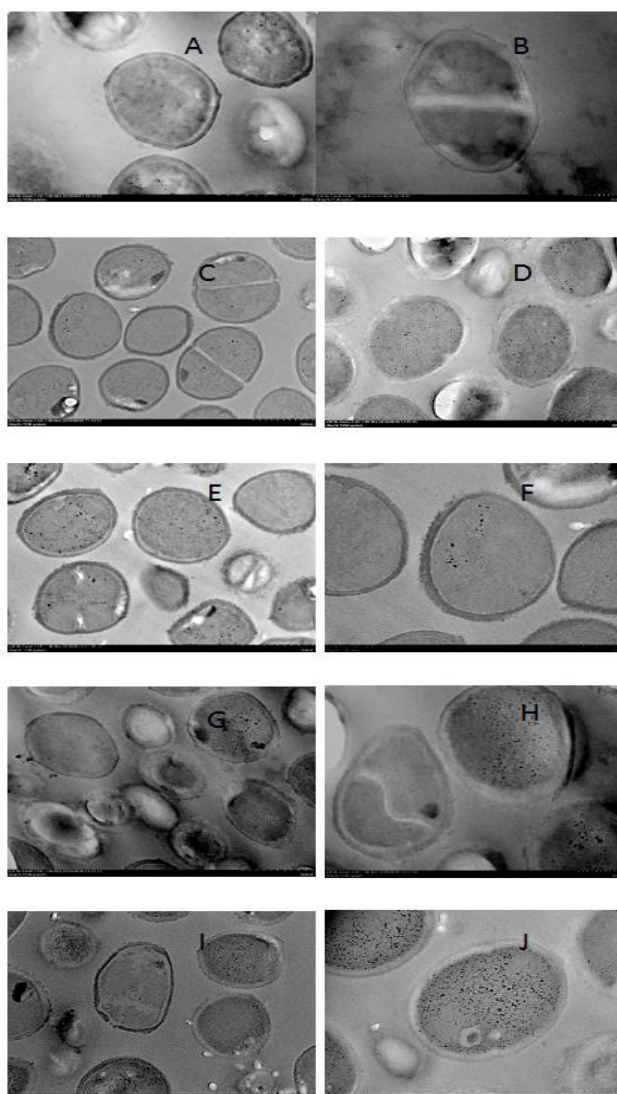


Fig.6. Transmission electron microscopy (TEM) of *S. aureus* ATCC 29213 after 9 and 24 hours of exposition to 6-Bis[(tri-p-tolylphosphonio)methyl]-3-hydroxypyridin-1-ium trichloride (2a); A, B – no compounds (24 h); C - 1×MBC (9 h), D – 2×MBC (9 h); E, F – MIC (24 h), G, H – 1×MBC (24 h); I, J – 2×MBC (24 h). The bar of A, C, D, E, G, I is 500 nm, bar of B, F, H, J is 200 nm.

The untreated cells of *S. aureus* showed homogeneous electron density in both cytoplasm and cell wall. Their cell walls and membranes are intact, with a dense peptidoglycan layer (Fig. 6AB). The significant morphological changes were observed in *S. aureus* cells treated with already MIC of **2a**, despite of the viability of the cells (see Fig 2). Cells exhibited diffuse character of cell wall with protrusions; the dividing cells have truncated or damaged separation membrane (compare Fig 6 B and F).

In presence of 1×MBC and 2×MBC cells are elongated and organized in chains (Fig 6 G-I); the cytoplasm is inhomogenous as compared to the control, the cell wall becomes more diffuse and crumble with visible areas of damage (Fig. 6H, J). The localized separation of the cell membrane from the cell wall could be observed (Fig. 6 C-J). The TEM images show that cells exposed to 1×MBC and 2×MBC of **2a** for 9 h exhibit similar cell wall shapes as after 24h treatment, with a slightly lower effect.

DISCUSSION

Recently, we have described a novel promising chemotype of antibacterial agents, and the primary purpose of this work was to investigate the structure-activity relationships as well as the mechanisms of action of the lead compounds. We demonstrated that the replacement of phenyl substituent with the *p*-tolyl group in the bis-phosphonium salts of pyridine significantly increased the antimicrobial activity. Thus, the obtained MIC values for the lead compound **2a** were 1-2 order of magnitude lower than those of similar compound **2** carrying phenyl substituents at the phosphonium groups (Fig. 1, Table 1). These data are in agreement with our earlier observations which showed high activity of phosphonium salts of pyridoxine with *p*-tolyl groups against gram-positive bacteria [9, 16]. By the way, the introduction of the *p*-tolyl group instead of the phenyl moiety drastically increased the cytotoxicity of compounds over two orders of magnitude for **1** vs **1a** and by one order of magnitude for **2** vs **2a** [10]. The quaternary phosphonium and ammonium salts are believed to interact with bacterial cell wall and damage the membrane function [11]. Since the activity of **2a** is very weak against Gram negative *P.aeruginosa* and *K.pneumonia* with glycoprotein layers (see Table 1) in contrast to gram-positive *Staphylococci* with peptidoglycan cell wall, we suggested that *p*-tolyl group targets **2a** to the cell wall and probably enhances thereby the membrane damaging activity of phosphonium group, while phenyl moiety diminishes this interaction. To test this suggestion and check the membrane integrity we investigated the total dehydrogenase activity. It has been revealed the significant decrease of activity only at 16 µg/ml of **2a** that is four times higher than MIC suggesting that membrane stays intact until this concentration of **2a** (Fig 3). Moreover, the CLSM also showed only partial loss of membrane integrity at 1×MIC of **2a**; even at 1×MBC, 20% of cells with intact membrane were identified (Fig 4b) suggesting an idea that cell membrane is not the main target of **2a**. Taking in account that compound **2a** exhibited high activity only against gram-positive microorganisms, we assumed that the bacterial cell wall could be a primary molecular target for this compound which is consistent with earlier studies of tolyl-substituted phosphonium salts [9,16].

Both SEM and TEM data identified significant truncations of the cell wall in the presence of **2a**, although without the leakage of the intracellular substances (see Figs. 5 and 6, respectively). The pronounced anomalies in the *S. aureus* cell structure treated by sub-lethal and lethal concentrations of bis-phosphonium salt **2a** suggest the damage of the cell-wall material that likely led to filamentous growth and excrescences and formation of unusual protrusions of cell surfaces (Fig. 5). The shapeless organic material observed on cell surfaces (Fig. 5F) seems to be a consequence of a loosened cell wall as determined by TEM (Fig. 6). Taken together, these data indicate that cell membrane remains almost intact at MIC of **2a** and confirm the idea that cell wall is a primary target of the compound. The cell death observed in time-kill curves and CLSM at 1×MBC and 2×MBC (Figs 3 and 4) could be related with significant damage of cell wall followed by the loss of membrane function and cell lysis. This mechanism differs from those of surfactants like quaternary ammonium salts which integrate into the cellular membrane and disrupt it by formation of pores [17,516].

In conclusion, our results demonstrate that the studied bis-phosphonium salt exerts the antimicrobial activity by causing cell wall damage, making this chemotype a promising starting point for the development of new antibacterial therapies.

ACKNOWLEDGMENTS

This work was supported by Program of Competitive Growth of Kazan Federal University.

REFERENCES

- [1] Pawlowski AC, Johnson JW, Wright GD. *Current Opinion in Biotechnology*, 2016; 42:108-117.
- [2] Rideout DC, Calogeropoulou T, Jaworski JS, Dagnino RJ, McCarthy MR. *Anti-Cancer Drug Design*, 1989; 4:265-280.
- [3] Romanov GV, Pozdeev OK, Gilmanova GKh, Ryzhikova Ya, Semkina EP. *Pharmaceutical Chemistry Journal*, 1990; 24:414-417.
- [4] Taladriz A, Healy A, Perez EJF, Garcia VH, Martinez CR, Alkhalidi AAM, Eze AA, Kaiser M, de Koning HP, Chana A, Dardonville C. *Journal of Medicinal Chemistry*, 2012; 55:2606-2622.
- [5] Galkina I, Bakhtiyarova Yu, Andriyashin V, Galkin V, Cherkasov R. *Phosphorus Sulfur and Silicon and the Related Elements*, 2013; 188:15-18.
- [6] Nagarajan N, Vanitha G, Ananth DA, Rameshkumar A, Sivasudha T, Renganathan R. *Journal of Photochemistry and Photobiology B: Biology*, 2013; 127:212-222.
- [7] Kanazava A, Ikeda T, Endo T. *Antimicrobial Agents and Chemotherapy*, 1994; 38:945-952.
- [8] Pugachev MV, Shtyrlin NV, Nikitina EV, Sysoeva LP, Abdullin TI, Iksanova AG, Ilaeva AA, Berdnikov EA, Musin RZ, Shtyrlin YuG. *Bioorganic and Medicinal Chemistry*, 2013; 21:4388-4395.
- [9] Pugachev MV, Shtyrlin NV, Sapognikov SV, Sysoeva LP, Iksanova AG, Nikitina EV, Musin RZ, Lodochnikova OA, Berdnikov EA, Shtyrlin YuG. *Bioorganic and Medicinal Chemistry*, 2013; 21:7330-7341.
- [10] Shtyrlin NV, Vafina RM, Pugachev MV, Khaziev RM, Nikitina EV, Zeldi MI, Iksanova AG, Shtyrlin YuG. *Russian chemical bulletin*, 2016; 65:535-545.
- [11] Timofeeva L, Kleshcheva N. *Applied Microbiology and Biotechnology*, 2011; 89: 475-492.
- [12] Kumar R, Banerjee AK. *Cellular and Molecular Life Sciences*, 1979; 35:160.
- [13] Rajvaidya N, Markandey DK. *Microbiology*, SB Nangia APH Publishing Corporation. New Delhi. 2006.
- [14] Aquino A, Chan J, Giolma K, Loh M. *Journal of Experimental Microbiology and Immunology*, 2010; 14:13-20.
- [15] Glauert AM, Lewis PR. *Biological Specimen Preparation for Transmission Electron Microscopy*, Portland Press Series. 1998.
- [16] Nikitina EV, Zeldi MI, Pugachev MV, Sapozhnikov SV, Shtyrlin NV, Kuznetsova SV, Evtygin VE, Bogachev MI, Kayumov AR, Shtyrlin YuG. *World Journal of Microbiology and Biotechnology*, 2016; 32:1-5.
- [17] Marcotte L, Barbeau J, Lafleur M. *Journal of Colloid and Interface Science*, 2005; 292:219-227.